Synthesis and Characterization of a Platinum(II) Complex Tethered to a Ligand of the Peripheral Benzodiazepine Receptor

Nicola Margiotta, Rosa Ostuni, Rosa Ranaldo, Nunzio Denora, Valentino Laquintana, Giuseppe Trapani, Gaetano Liso, and Giovanni Natile*

Dipartimento Farmaco-Chimico, Università degli Studi di Bari, Via E. Orabona 4, 70125 Bari, Italy

Received October 18, 2006

A peripheral benzodiazepine receptor (PBR) ligand (TZ6, **5**) has been selected as receptor-mediated carrier for antitumor cisplatin-like compounds. Compound **5**, containing a thiazole ring in position 2 of the imidazopyridine nucleus, is able to act as a dinitrogen chelate toward platinum. The resulting complex, *cis*-[$PtCl_2$(**5**)], that is, compound **8**, has been fully characterized by NMR techniques and has been shown to possess affinity and selectivity for the PBR comparable to those of **5** (IC_{50} of 4.6 and 2.81 nM for **8** and **5**, respectively; selectivity indexes for PBR greater than 10 000 for both compounds). Hence, a platinum moiety cross-linking the imidazopyridine and the thiazole aromatic rings does not alter the affinity for PBR. The same cross-linking could be responsible for the tendency of **8** to associate in dimers. The equilibrium between monomer and dimer has been investigated by NMR spectroscopy and the corresponding constant determined.

Introduction

Since 1978, *cis*-diamminedichloroplatinum(II) (cisplatin) has become one of the five antitumoral agents most used in clinical therapy.[1] Its effectiveness is limited by two factors: toxicity (ototoxicity, neuropathy, myelosuppression, renal, and hepatic toxicity) and intrinsic or acquired resistance. Intrinsic resistance is responsible for the limited spectrum of activity of cisplatin, which is used mainly in the treatment of ovarian, head and neck, bladder, and testicle tumors.[2,3] The search for cisplatin analogues with better pharmacological properties has involved many research groups in the last three decades. Although the structure−activity relationships of platinum antitumoral drugs, as described by Cleare and Hoeschele,[4,5] have inspired the synthesis of many of the new platinum compounds, some platinum compounds that do not fulfill at least one of the classic structure−activity relationships ("nonclassic" platinum drugs) have been investigated and some of them demonstrated good antineoplastic activity also in vivo, hence opening the way to new generation platinum drugs.[6−8]

The design of new platinum compounds has also involved the use of biologically active carrier ligands such as DNA intercalators, doxorubicin, estrogen analogues, aminoacids, ferrocene, phosphonates, and sugars.[6,9,10] These ligands have been selected as molecular carriers to obtain a specific delivery and accumulation of the antitumor drug to the target cells or organs (drug targeting and delivery) or synergistic pharmacological activities.

Pursuing our interest for tissue-specific targeting of complexes, we have attempted the synthesis of platinum compounds with ligands specific for the peripheral benzodiazepine receptor (PBR) such as 2-[6,8-dichloro-2-(1,3-thiazol-2-yl)*H*-imidazo-[1,2-*a*]pyridin-3-yl]-*N*,*N*-dipropylacetamide (TZ6, **5**, Chart 1). PBRs, for which the name "translocator protein" has recently been proposed,[11] are abundant in peripheral tissues and also in glial cells of the central nervous system (CNS). They are located primarily on the outer mitochondrial membrane and are involved in a functional structure, designated as mitochondrial permeability transition (MPT) pore, which controls apoptosis.[12] Opening of the MPT pore induces apoptosis, whereas pharmacological inhibition of this pore prevents cell death. Moreover, there is overwhelming evidence that PBRs are involved in the regulation of cholesterol transport and that activation of these receptors stimulates the synthesis of neuroactive steroids.[13] Our choice of PBR-binding ligands for targeting purposes stems also from the observation that an overexpression of PBRs occurs in many tumor types,[14,15] such as brain, liver, hepatic, glial, and mammary tumors, breast carcinoma, and ovarian and colorectal cancers. Furthermore, the grade of overexpression of PBR appears to be correlated with the malignancy of the tumor.[16] Attempts to select PBR-binding ligands as receptor-mediated carriers for antitumoral drugs have already been made.[17] A reported proof of the concept is the conjugation of the isoquinolinecarboxamide derivative PK11195 (1-(2-chlorophenyl)-*N*-methyl-*N*-(1-methyl-propyl)-3-isoquinoline carboxamide, a ligand having high affinity and selectivity for PBR) with the antineoplastic drug gemcitabine.[18,19] More recently, the potential

Chart 1. Sketches of Alpidem, Zolpidem, and Compound **5** (TZ6)

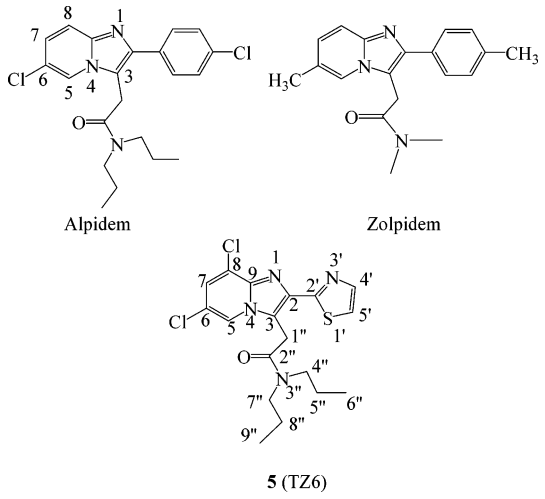

* To whom correspondence should be addressed. Phone: +39 080 5442774. Fax: +39 080 5442230. E-mail: natile@farmchim.uniba.it.

10.1021/jm0612160 CCC: $37.00 © 2007 American Chemical Society
Published on Web 02/08/2007

of the strategy to use PBR ligands as carriers for antitumor agents has been demonstrated in in vivo studies. Thus, it has been shown that Ro5-4864 (7-chloro-5-(4-chlorophenyl)-1,3-dihydro-1-methyl-2*H*-1,4-benzodiazepin-2-one, 4′-chlorodiazepam) potentiates tumor growth inhibition induced by etoposide (or a combination of etoposide and ifosfamide) in small lung cancer xenografts.[20] It has also been shown that diazepam cooperates with lonidamine to inhibit growth of human glioblastoma xenografts.[21] Altogether, these findings suggest that PBR ligands could be used for chemosensitization of solid tumors. Moreover, it has been demonstrated that PBR ligands can also cause dissipation of the inner mitochondrial transmembrane potential ($\Delta\psi_m$) leading to the release of apoptogenic factors such as the apoptosis-inducing factor.[20] Hence, conjugation of PBR ligands with antitumor drugs may increase their efficacy toward tumors.

Compounds endowed with high affinity and selectivity for PBR have been obtained by structural modification of the 2-phenylimidazopyridine acetamides alpidem and zolpidem (Chart 1).[22−24] One of these derivatives is compound **5**, which is characterized by a thiazole ring in position 2 of the imidazopyridine nucleus and, therefore, can be considered a thiazole analogue of alpidem and zolpidem.

We report here on the synthesis and characterization of a platinum complex having **5** as a carrier ligand, which could combine the alkylating properties derived from the metal core with the high affinity of **5** for tissues overexpressing PBR. Chelation of **5** to platinum would also allow the formation of a large planar aromatic polycyclic system that could have intercalative properties into the DNA molecule (another feature that could circumvent cisplatin resistance).[25] Furthermore, the high lipophilicity of the imidazopyridine and thiazole rings might allow the complex to cross the blood−brain barrier (BBB) and be effective against tumors of the CNS. The chemical behavior of the newly synthesized compound in solvents with different dielectric constants has also been investigated. Preliminary binding assays have shown that the newly prepared platinum complex maintains the high affinity and selectivity for PBR typical of **5**.

Scheme 1. Synthesis of **5**[a]

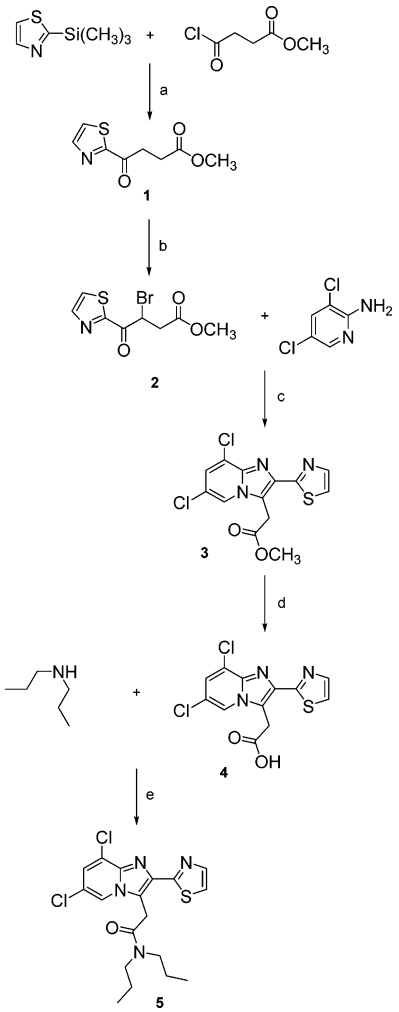

[a] Reagents and conditions: (a) 0 °C ; (b) $PyH^+Br_3^-$/THF; (c) toluene, △; (d) dioxane, HCl 1 N; (e) EEDQ/THF.

Results and Discussion

Compound **5** has two soft donor atoms that can coordinate to platinum:[26−28] the N(1) of the imidazo-pyridine system and the N(3′) of the thiazole-ring (Chart 1). These two donor atoms can coordinate to platinum from *cis* positions, the resulting *N*,*N*-chelation leading to formation of a stable five-membered ring. It has already been shown that the sulfur atom of thiazole has negligible coordinating ability for platinum.[28]

Compound **5** was prepared by the sequence of reactions reported in Scheme 1, which contemplates the synthesis of the methyl bromoester **2** by a reported procedure,[29] followed by its condensation with 3,5-dichloro-2-amino-pyridine to give, after hydrolysis, the 2-thiazolylimidazopyridine-acetic acid **4**, which finally is condensed with dipropylamine.

A thorough characterization of **5** was accomplished by one-dimensional (1D) ^{1}H (acetone-d_6 and $CDCl_3$) and ^{13}C ($CDCl_3$), two-dimensional (2D) COSY, and [^{1}H−^{13}C]-HETCOR ($CDCl_3$) NMR spectroscopy. The values of the ^{1}H and ^{13}C chemical shifts are reported in Table 1. The ^{1}H NMR 1D (top) and 2D COSY (bottom) spectra of **5** in acetone-*d*6 are reported in Figure 1. The doublets at 8.66 and 7.53 ppm have coupling constants (1.82 Hz) typical for two protons in *meta* positions, therefore, they were assigned to the two protons of the imidazopyridine moiety. In particular, the less shielded signal at 8.66 ppm was assigned to H(5), which, differently from H(7), is flanked by an electronegative nitrogen atom. Consequently, the signal at 7.53 ppm was assigned to H(7) (this assignment of the aromatic protons was also supported by a NOESY experiment showing a cross-peak between the signal at 8.66 ppm and the signal of the methylene protons H(1″), see following discussion). The doublets at 7.94 and 7.68 ppm exhibit a coupling constant of 3.6 Hz, which is typical of two protons in *ortho* positions, therefore, they were assigned to the two protons of the thiazole ring. Also in this case, according to literature data,[30] the more downfield doublet at 7.94 ppm was assigned to proton H(4′), which is flanked by a nitrogen atom. The singlet at 4.85 ppm was assigned to the isolated methylene protons H(1″). The signals of the two propyl substituents were assigned with the help of a 2D-NOESY experiment (Figure 2). The two propyl substituents are not equivalent because of restricted rotation about C(2″)−N(3″), which has a partial double-bond character. Two cross-peaks correlate the methylene protons H(1″) to the aromatic proton H(5) and to the triplet at 3.53 ppm, hence, the latter resonance has to be assigned to protons H(4″). The triplet belonging to protons H(4″) was also coupled to the multiplet at 1.74 ppm, which, consequently, was assigned to H(5″). Finally, the multiplet at 1.74 ppm was coupled with the triplet at 0.95 ppm, which was assigned to protons H(6″). The remaining set of signals at 3.29 ppm (triplet), 1.52 ppm (multiplet), and 0.81 ppm (triplet) with internal scalar (COSY)

Table 1. ^{1}H and ^{13}C (italics) NMR Chemical Shifts (ppm) for **5** and **8**[a]

cmpd	solvent	5	7	4′	5′	1″	4″	7″	5″	8″	6″	9″
5	acetone-d_6	8.66, d (1.82)	7.53, d (1.82)	7.94, d (3.60)	7.68, d (3.60)	4.85, s	3.53, t (7.82)	3.29, t (7.50)	1.74, ss (7.82)	1.52, ss (7.50)	0.95, t (7.37)	0.81, t (7.40)
8: monomer	acetone-d_6	8.73, d (1.63)	7.74, d (1.63)	8.13, d (3.50)	8.01, d (3.50)	4.89, s	3.59, t (7.78)	3.32, t (7.45)	1.87, ss (7.85)	1.56, ss (7.52)	1.07, t (7.29)	0.83, t (7.46)
5	$CDCl_3$	8.60, *122.9*	7.31, *125.7*	7.86, *143.5*	7.39, *119.8*	4.70, *30.3*	3.42, *50.0*	3.27, *48.3*	1.55,[b] *21.5*	1.55,[b] *21.5*	0.82, *11.2*	0.82, *11.2*
8: monomer	$CDCl_3$	8.15, br	7.75, br	8.70, d (3.60)	7.88, d (3.60)	4.36, s	3.42. t (7.50)	3.35. t (7.50)	1.80, br	1.56[b]	1.06, t (7.20)	0.89, t (7.20)
8: dimer	$CDCl_3$	7.99, br, *124.2*	7.35, br, *132.4*	7.96, br, *138.9*	7.46, br, *119.8*	4.78, s, *31.8*	3.52, br, *50.4*	3.28, t (7.20), *48.2*	1.80, br, *22.5*	1.56,[b] *20.8*	1.10, br, *11.5*	0.85, t (7.20), *11.5*

[a] Numbering is as reported in Chart 1. J_{H-H} are reported in parentheses; d = doublet, s = singlet, t = triplet, ss = sextet, br = broad. [b] Overlapping with the residual HDO signal.

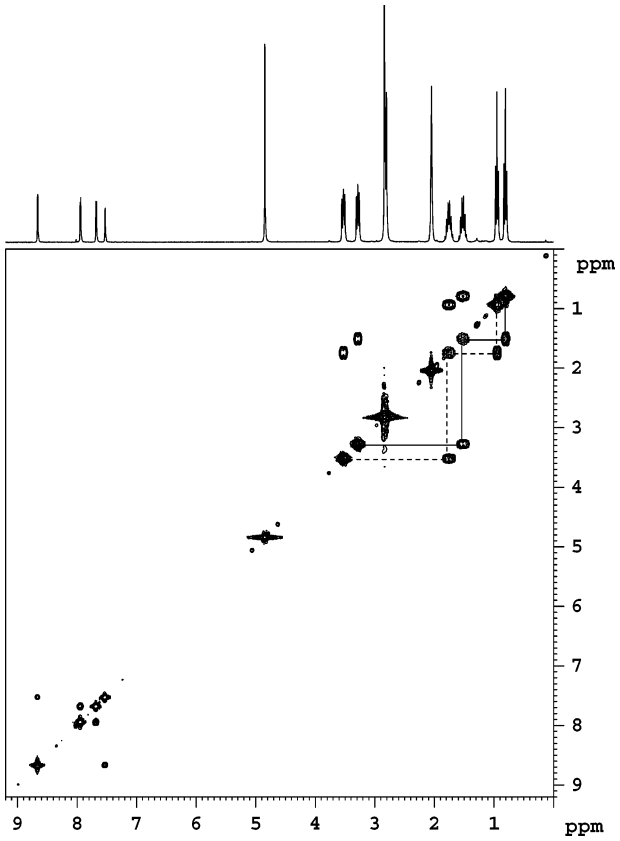

Figure 1. ^{1}H (top) and 2D COSY contour plot (bottom) of **5** in acetone-d_6.

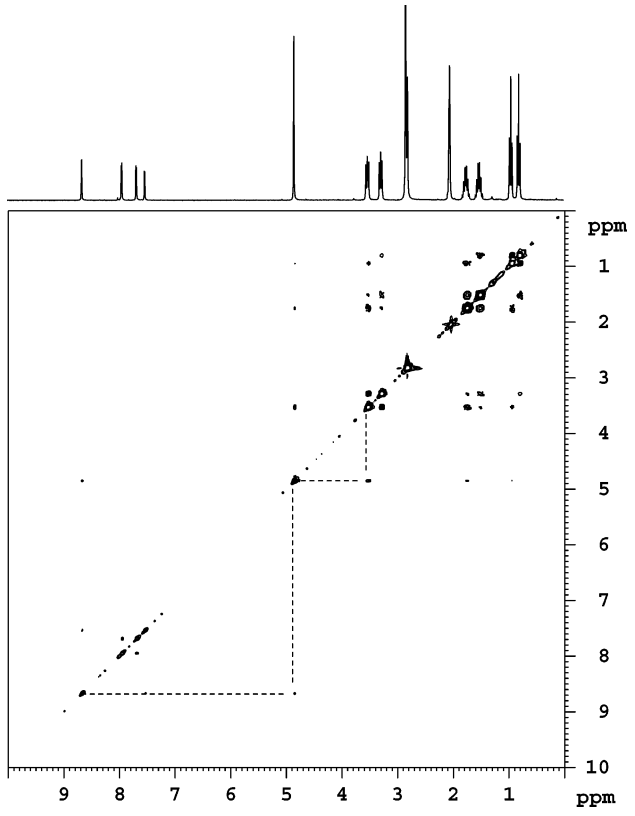

Figure 2. ^{1}H (top) and 2D NOESY contour plot (bottom) of **5** in acetone-d_6.

Scheme 2. Synthesis of Compound **8**[a]

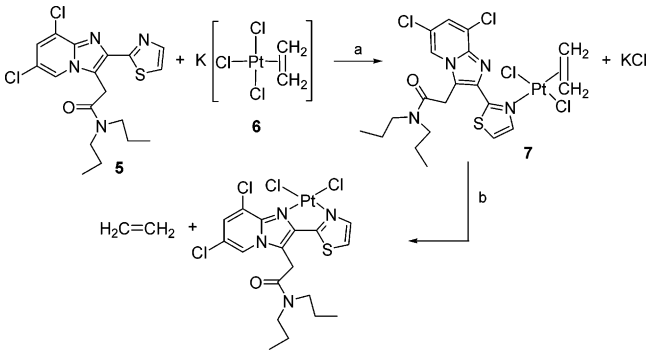

[a] Reagents and conditions: (a) MeOH, 24 h; (b) $CHCl_3$, 50 °C, 7 days.

and spatial (NOESY) couplings was assigned to the second propyl chain (protons H(7″), H(8″), and H(9″), respectively). The latter propyl chain appears to be more shielded than the former one, probably because of the vicinity of the carbonyl group of the amidic functionality.[31] Molecular modeling of compound **5** showed that the distances between protons H(1″)/H(5) and H(1″)/H(4″) are in the range of values detectable with a 2D-NOESY experiment (ca. 4 Å).[32]

The ^{13}C NMR chemical shifts of **5** were obtained by a [$^{1}H-^{13}C$]-HETCOR 2D-NMR experiment (Figure S1 in Supporting Information). As expected, carbon C(4′) (143.5 ppm), adjacent to the more electronegative nitrogen atom N(3′), was less shielded than C(5′) (119.8 ppm) adjacent to a sulfur atom, while the carbon atom C(5) (122.9 ppm) resulted to be more shielded than C(7) (125.7 ppm), with this latter being influenced by the presence of two adjacent chlorine atoms.

The platinum complex *trans*-[$PtCl_2(C_2H_4)$(**5**)] (**7**, Scheme 2) was synthesized by the reaction of **5** with Zeise's salt K[$PtCl_3$-(η^2-C_2H_4)] (**6**). The latter substrate is characterized by a high reactivity originated by the presence of an ethylene ligand that exerts a strong labilizing effect on the *trans* ligand. The reaction

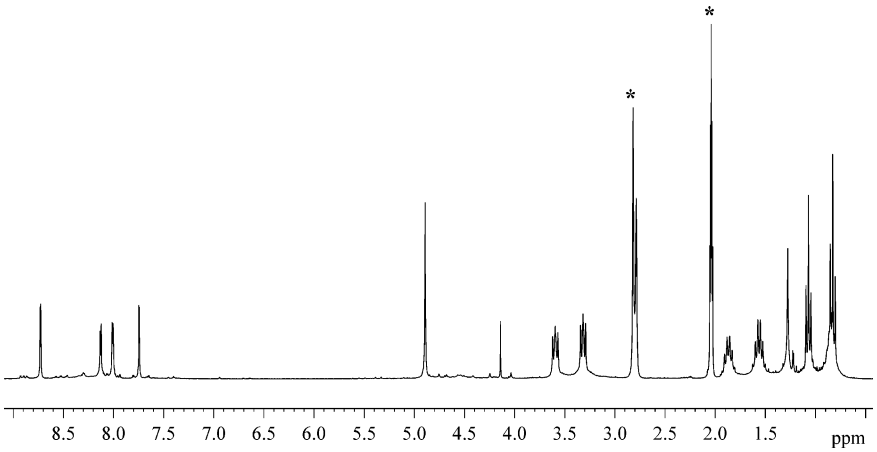

Figure 3. ^{1}H NMR (acetone-d_6) spectrum of **8**. The complex concentration is about 1.0×10^{-3} M. The asterisks indicate solvent signals.

leads to formation of a reaction product (**7**) in which **5** is monocoordinated and has displaced the chlorido ligand *trans* to ethylene.

The IR spectrum of **7** exhibits only one signal in the region of Pt−Cl stretchings (332.2 cm^{-1}), which is typical of platinum compounds with two chlorido ligands in *trans* positions. The ^{1}H NMR spectrum in $CDCl_3$ has a signal at 4.57 ppm, flanked by platinum satellites ($^2J_{H-Pt} \sim 60$ Hz), which is typical of a Pt-coordinated ethylene in a square planar complex.[33] A doublet at 8.04 ppm with Pt-satellites ($^3J_{H-Pt} \sim 40$ Hz, typical of a thiazole N-coordinated)[34] is assigned to proton H(4′) (a 2D COSY experiment confirms this assignment; data not shown) and supports coordination of platinum to N(3′).

The initially formed compound **7** containing monocoordinated ligand **5** slowly (stirring in chloroform solution at 50 °C for one week) evolves to a new species, *cis*-[$PtCl_2$(**5**)] (complex **8**, Scheme 2), containing biscoordinated ligand **5**.

The IR spectrum of **8** showed two signals (351.8 and 335.2 cm^{-1}) in the region of Pt−Cl stretchings, which are characteristic of a *cis*-$PtCl_2$ moiety. The amide carbonyl stretching (1636 cm^{-1}) is shifted to lower wave numbers as compared to the analogous stretching in free **5** (1649 cm^{-1}).

The ^{1}H spectrum of **8** (acetone-d_6, complex concentration ca. 10^{-3} M) is reported in Figure 3, while the ^{1}H and ^{13}C chemical shifts are reported in Table 1. Comparison of ^{1}H NMR spectra (acetone solution) for free and complexed ligand **5** shows that, as expected upon coordination to platinum, the thiazole and imidazole protons undergo a significant deshielding (downfield shifts of 0.07, 0.21, 0.19, and 0.33 ppm for H(5), H(7), H(4′), and H(5′), respectively).

Contrary to the case of the acetone-d_6 solution, in $CDCl_3$ the complexed species **8** exhibits two sets of signals in the ^{1}H NMR spectrum whose relative ratio changes with the complex concentration (Figure 4) and which have been assigned to a monomeric and a dimeric species. One species (presumably the monomer) is favored at low concentration and becomes almost the exclusive form at a concentration $<10^{-4}$ M. In contrast, the second species (presumably a dimer) is favored at high concentration and becomes highly dominant at concentration $>10^{-3}$ M. A major difference between monomer and dimer is that the latter has all aromatic protons undergoing an upfield shift, which is highest for H(4′) (0.74 ppm, Table 1) and lowest for H(5) (0.16 ppm).

The full NMR characterization of the proposed dimeric species was accomplished with the help of 2D [^{1}H−^{13}C] HETCOR (Figure S3), TOCSY (Figure S4), and ROESY (Figure S5) experiments (the latter two were particularly useful for assigning protons of the propyl chains) performed on concentrated (10^{-3} M) $CDCl_3$ solutions. For the same solution, the ^{195}Pt NMR spectrum (Figure 5) showed one broad signal at −2012 ppm falling in the range typical for a platinum atom in a Cl_2N_2 coordination environment (the quadrupolar effect of ^{14}N being responsible for the broadening of the signal). The

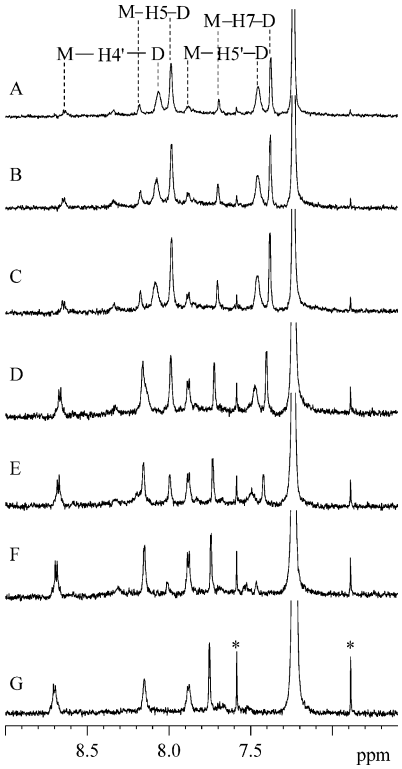

Figure 4. ^{1}H NMR spectra of a sample of compound **8** in $CDCl_3$ recorded at the following total concentrations: A, 8.8×10^{-4} M; B, 7.4×10^{-4} M; C, 5.3×10^{-4} M; D, 3.3×10^{-4} M; E, 2.4×10^{-4} M; F, 1.4×10^{-4} M; G, 0.7×10^{-4} M. Signals relative to protons of the monomeric and dimeric species are indicated with M and D, respectively. The asterisks indicate the satellites due to the coupling with ^{13}C of the $CDCl_3$ residual proton signal.

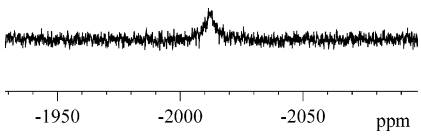

Figure 5. ^{195}Pt NMR spectrum ($CDCl_3$, complex concentration of about 1.0×10^{-3} M) of the dimeric species of compound **8**.

Table 2. Intensities of NMR Signals (I_M and I_D, normalized to 10), Concentration of Species ([*M*] and [*D*]), and Evaluated Values of *K*[a]

C_{TOT} (M)	I_D	I_M	[*M*] (M)	[*D*] (M)	*K* (M^{-1})
1.1×10^{-3}	6.47	3.53	3.92×10^{-4}	3.59×10^{-4}	2338.59
8.8×10^{-4}	6.32	3.68	3.26×10^{-4}	2.80×10^{-4}	2635.95
7.4×10^{-4}	6.03	3.97	2.93×10^{-4}	2.22×10^{-4}	2590.62
5.3×10^{-4}	6.06	3.94	2.09×10^{-4}	1.61×10^{-4}	3665.63
3.3×10^{-4}	4.62	5.38	1.79×10^{-4}	7.66×10^{-5}	2397.34
2.4×10^{-4}	3.92	6.08	1.44×10^{-4}	4.64×10^{-5}	2236.04
1.4×10^{-4}	3.00	7.00	9.94×10^{-5}	2.13×10^{-5}	2155.79

[a] $K = [D]/[M]^2$; C_{TOT} = total concentration of starting compound **8** in $CDCl_3$ solution; [*D*] = concentration of the dimer; and [*M*] = concentration of the monomer.

small concentration required for having the monomeric species dominating in solution did not allow detection of its ^{195}Pt signal.

Several platinum(II)−diimine complexes have shown a tendency to arrange, mainly in the solid state but also in solution, in piles with stacking Pt(II) square planar monomeric units.[35] An historical example is [$PtCl_2$(bipy)] (bipy = 2,2′-bipyridyl), which exists in two polymorphic forms: the yellow and the red forms. The square planar complexes of the red form stack to form an approximately linear Pt···Pt chain with a spacing of 3.45 Å. Although the latter is a less efficient mode of packing as compared to the yellow polymorph, nevertheless it is promoted by specific attractions between chlorido ligands and aromatic heterocycles and between platinum atoms of adjacent units.[36,37]

The two species present in equilibrium in chloroform solutions of **8** have been assumed to be a monomer and a dimer. This assumption is supported by the observation that the species dominating at low concentration ($<10^{-4}$ M) has a ^1H NMR spectrum (Figure 4, spectrum G) very similar to that recorded for compound **8** in acetone-d_6 (Figure 3), where the concentration has no influence on the spectrum and the large dielectric constant (far greater than that of chloroform) weakens intermolecular interactions. The species dominating at high concentration ($>10^{-3}$ M) has been assumed to be a dimer because this is the simplest aggregate one can think of. However, we can anticipate that diffusion ordered NMR spectroscopy (DOSY) experiments (reported later in the discussion) fully support the latter assumption.

From the concentrations of the two forms (Table 2) it has been possible to estimate the constant for the equilibrium monomer/dimer ($K = [D]/[M]^2$). The resulting values (Table 2) are fairly constant in the range of concentrations explored and give an average value of 2.57 (± 0.51) × 10^3 M^{-1}. Such an equilibrium constant is in agreement with data reported in the literature for similar processes in which, however, the interconversion between monomer and dimer was fast in the NMR time scale and only one set of signals, which was the coalescence of the signals of individual species, was observed in the NMR spectrum.[38,39] It is suggested that in the dimeric species the two molecules are oriented in opposite directions and stacked in an antiparallel fashion.[40] Such an arrangement would bring the two chlorido ligands of one subunit above the planar heterocyclic system of the second subunit and close to the H(7)/H(5) and H(4′)/H(5′) atoms which, therefore, experience a shielding effect as revealed by the NMR spectra. Our hypothesis is also supported by geometry optimization experiments in the gas phase performed at the PM3 level starting from a dimeric model in which the two units were placed at a Pt···Pt distance of 3.5 Å. The resulting molecular model is reported in Figure 6. From this model it appears that the two units are held together by interactions between the coordinated chlorido ligands and the imidazo-pyridine cycle, while the two Pt atoms are at a distance of 3.91 Å.

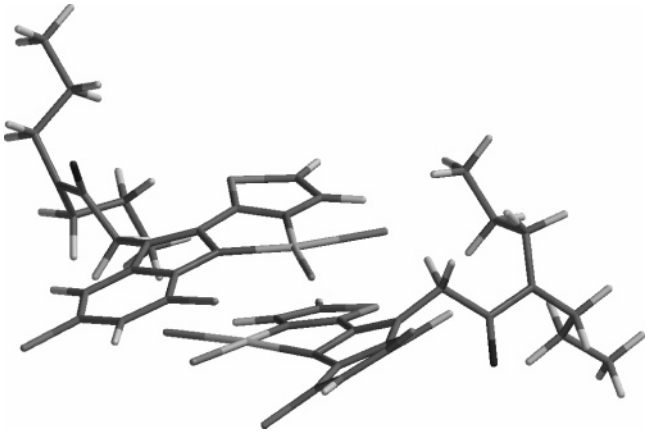

Figure 6. Gas-phase optimized (PM3 level) structure of the dimeric aggregate formed by complex **8** in $CDCl_3$ at high concentration.

To confirm that the equilibrium involves monomeric and dimeric species, we performed DOSY experiments to evaluate the corresponding translational diffusion coefficients (Diff). Such a technique has proven to be very useful in the determination of the molecular size of organometallic compounds.[41,42] For the monomeric species the DOSY experiment was performed on a diluted sample of **8** (1.0×10^{-4} M in $CDCl_3$, Figure 7). Integrals and intensities of selected peaks were quantified with the Bruker T1/T2 software package and fitted to the Stejskal-Tanner equation[43,44] leading to a Diff of 1.33 (±0.06) × 10^{-9} m^2 s^{-1} (Table 3). This experimental value was compared to the theoretical Diff of monomeric **8** calculated using the Stokes−Einstein equation. For the above calculation, the viscosity of the chloroform solution of **8** was approximized to that of the pure solvent at the same temperature, while the radius of the molecular sphere was taken equal to that calculated from a gas-phase structure of **8** optimized at the PM3 level (r = 4.88 Å). Moreover, because for molecules with van der Waals radii <5 Å the Stokes−Einstein factor of 6 can be changed to 4,[45] we adopted the latter value for our calculations. The theoretical Diff resulted to be 1.24×10^{-9} m^2 s^{-1}, which is quite close to the Diff found experimentally, thus confirming the presence of monomeric units in dilute solutions.

A second DOSY experiment was performed on a concentrated sample of **8** (ca. 1.0×10^{-3} M in $CDCl_3$, not shown) using the same conditions as for the previous experiment. The measured Diff was 9.87 (± 0.21) × 10^{-10} m^2 s^{-1} (Table 3). Also, for the dimer, the experimentally determined Diff is almost coincident with the calculated one (9.89×10^{-10} m^2 s^{-1}, Table 3).

As expected, the Diff for the proposed dimeric species is smaller than that of the monomer, with the ratio Diff(monomer)/Diff(dimer) being 1.34. This result is in line with other literature data such as that concerning dimeric and tetrameric THF-solvated *n*-butyllithium aggregates.[42] For the latter case, the ratio between the experimentally determined Diff of the dimeric and tetrameric species was ca. 1.14. It is worth noting that, because complex **8** has a nonspherical shape, it is not possible to think of a dimeric species as a sphere having a volume double that of the monomer. Therefore, a relative Diff of 1.34 fully supports the proposed equilibrium between monomeric and dimeric species.

It should also be noted that free ligand **5** does not undergo the dimerization process observed for its platinum derivative when dissolved in $CDCl_3$. A major difference between free and complexed **5** is the coplanarity of the thiazole and imidazopy-

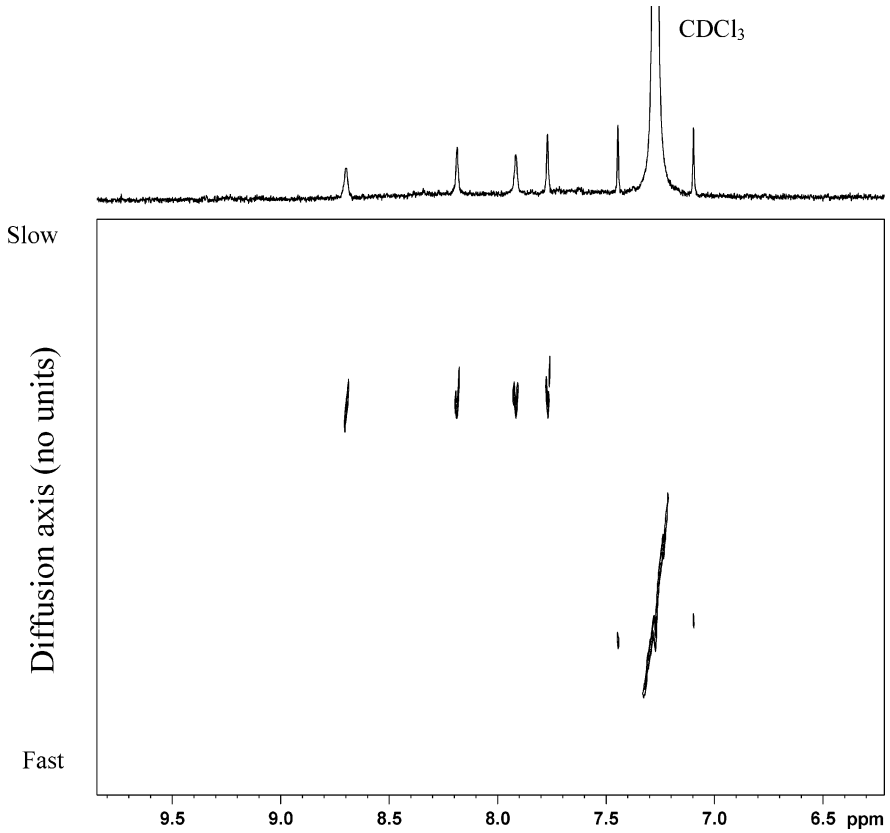

Figure 7. 2D diffusion ordered ^{1}H spectrum (DOSY) of complex **8** in $CDCl_3$ at 298 K; complex concentration of about 1×10^{-4} M.

Table 3. Calculated and Measured Diff ($m^2\ s^{-1}$) for Compound **8** in $CDCl_3$ Solutions at 298 K

	calculated[b]	experimental[c]
monomer[a]	1.24×10^{-9}	$1.33\ (\pm 0.06) \times 10^{-9}$
dimer[d]	9.89×10^{-10}	$9.87\ (\pm 0.21) \times 10^{-10}$

[a] Concentration = 1.0×10^{-4} M. [b] Calculated from the Stokes−Einstein equation. [c] Obtained as the average value with standard deviation from independent Diff values determined for five different NMR signals of each species. [d] Concentration = 1.0×10^{-3} M.

ridine rings imposed by the platinum cross-link. Therefore, it is most likely that the free rotation of the thiazole ring (about the C(2)−C(2′) bond) in free **5** destabilizes the planar conformation, preventing the stacking of two molecules in a dimer. It is also possible that in the complexed species a key role in the stabilization of the dimeric species is played by the interaction between chlorido ligands of one subunit and aromatic thiazole and imidazopyridine rings of the second unit.[46]

Because one of the aims of this study was to prepare a platinum complex specific for those tumors overexpressing the PBR, the affinity of the complexed species **8** for PBR was evaluated by measuring its ability to displace [^{3}H]PK 11195 from binding to membrane preparations of the cerebral cortex. We can anticipate that the platinum complex has PBR affinity comparable to that of free **5** (IC_{50} of 4.6 and 2.81 nM for **8** and **5**, respectively). Both of these compounds also possess high selectivity for PBR, showing selectivity indexes (defined as the ratio IC_{50} CBR/IC_{50} PBR) greater than 10 000. In previous reports it was shown how both the substituent at C(2) of the imidazopyridine nucleus and the substituent on the carboxamide nitrogen have a relevant influence on the binding affinity of **5** for PBR.[22−24] The present results indicate from a structure−affinity point of view that a platinum moiety cross-linking the imidazopyridine and the thiazole aromatic rings and imposing a planar conformation does not alter the affinity for PBR.

Conclusions

In this work, a platinum(II) complex (**8**) containing a ligand with high affinity for PBR (**5**) has been successfully synthesized. NMR techniques (^{1}H and ^{195}Pt{^{1}H} 1D, ^{1}H COSY, TOCSY, NOESY, DOSY, and [^{1}H−^{13}C] HETCOR 2D experiments) have allowed the full characterization of the complex stereochemistry and unraveled the property of this new platinum complex to undergo dimerization in solvents with low dielectric constants via formation of noncovalent intermolecular interactions. The formation of such an aggregate appears to be promoted by the extensive planar aromatic moiety that is formed once the platinum is coordinated to **5**. Such a property can forsee an intercalating ability of this platinum complex toward DNA. This latter property is absent in the case of cisplatin. Compound **8**, like similar complexes of platinum with sterically hindered heterocyclic ligands,[47] has a poor solubility in water, however, its greater lipophilicity (as compared to cisplatin) might favor the BBB penetration. In any case, we are seeking the preparation of more water soluble analogues of **8** by exchanging the chlorido ligands for carboxylate and related ligands.

Of great relevance is the high affinity of **8** for the PBR, which makes this compound a potential selective drug for tumors at the brain level. The investigation of the antitumor activity of **8** is under way.

Experimental Section

Chemicals. 2-Trimethylsilylthiazole was purchased from Lancaster Synthesis, Ltd. (Milan, Italy), and 3-methoxycarbonylpropionyl chloride, pyridinium bromide perbromide, ethyl 1,2-dihydro-2-ethoxy-1-quinolinecarboxylate (EEDQ), and 2-amino-3,5-dichloropyridine were purchased from Sigma-Aldrich (Milan, Italy).

Commercial reagent grade chemicals and solvents were used without further purification.

Instrumental Measurements. Melting points were determined in open capillary tubes with a Büchi apparatus and are uncorrected.

IR spectra were obtained on a Perkin-Elmer IR Fourier transform spectrophotometer in KBr pellets. ^{1}H NMR spectra were recorded on Varian VX Mercury and Bruker Avance DPX instruments, both operating at 300 MHz. Standard pulse sequences were used for ^{1}H, ^{13}C{^{1}H}, and ^{195}Pt{^{1}H} 1D spectra. The COSY, TOCSY, [^{1}H-^{13}C] HETCOR, and NOESY 2D experiments were carried out using gradient selected versions of the standard Bruker pulse programs. Chemical shifts are given in δ values. ^{1}H and ^{13}C chemical shifts were referenced to TMS by using the residual protic peak of the solvent as internal reference: 2.04 ppm (^{1}H) for acetone-d_6; 2.55 ppm (^{1}H) for DMSO-d_6, and 7.23 ppm (^{1}H) and 77.7 ppm (^{13}C) for $CDCl_3$. ^{195}Pt chemical shifts were referenced to external K_2-[$PtCl_4$] in D_2O fixed at −1615 ppm. DOSY experiments[44,48,49] were carried out on a Bruker Avance II 600 spectrometer operating at 600 MHz and equipped with a GAB gradient unit. A standard Bruker stimulated echo sequence with bipolar gradient pulses for diffusion and one spoil gradient was used with a ramp of 64 different gradient strengths (0.674−32.030 G cm^{-1}) of 1.5 ms duration (δ), diffusion times (Δ) of 0.100 s (32 scans), and a relaxation delay of 1.5 s. Integral and peak intensities were processed with the Bruker T1/T2 relaxation processing included in TOPSPIN software package (version 1.3).

Mass spectra were recorded on a Hewlett-Packard 5995c GS-MS low-resolution spectrometer and an Agilent 1100 LC-MSD trap system VL instrument using methanol/ammonium formiate 7 mM (water solution) 9:1 (v/v). Elemental analyses were carried out with a Hewlett-Packard 185 C, H, and N analyzer.

The reactions for the preparation of **5** were performed under a nitrogen atmosphere. The progress of the reaction was monitored by thin-layer chromatography (TLC) on Kieselgel 60 F254 (Merck). Solvents were evaporated under reduced pressure with a rotary evaporator. Compounds **1**−**5** were purified on column chromatography using silica gel 60 (Merck 70−230 mesh).

Synthesis of 2-[6,8-Dichloro-2-(1,3-thiazol-2-yl)*H*-imidazo[1,2-*a*]pyridin-3-yl]-*N*,*N*-dipropylacetamide (5). The synthesis of compound **5** was accomplished starting from 3-methoxycarbonylpropionyl chloride through a five-step process.

Step 1: Preparation of Methyl 4-Oxo-4-(1,3-thiazol-2-yl)-butanoate (1). Compound **1** was synthesized using a previously reported method.[29] Briefly, 2-trimethylsilylthiazole (1.00 mL, 6 mmol) was added slowly and under stirring to 1.54 mL (12 mmol) of 3-methoxycarbonylpropionyl chloride kept at 0 °C. The stirring was continued at room temperature for 15 h, then the crude mixture was treated with diethyl ether (2 × 50 mL) and $NaHCO_3$ (2 × 50 mL of a saturated water solution). The organic layer was removed, dried (Na_2SO_4), and taken to dryness under vacuum. The residue was purified by column chromatography on silica gel (petroleum ether/ethyl acetate 6:4 v/v as eluent) to give 0.70 g (58% yield) of compound **1** as a yellow oily residue.

Step 2: Preparation of Methyl 3-Bromo-4-oxo-4-(1,3-thiazol-2-yl)butanoate (2). Also the preparation of compound **2** has already been reported.[29] Briefly, pyridinium bromide perbromide (3.37 g, 10.55 mmol) was added to a stirred solution of **1** (2.00 g, 10.55 mmol) in anhydrous THF (40 mL). The reaction mixture was stirred under N_2 for 12 h at 40−60 °C. The solvent was removed under reduced pressure, and the resulting residue was treated with diethyl ether (2 × 50 mL) and $NaHCO_3$ (2 × 50 mL of a saturated water solution). The organic layer was removed, dried (Na_2SO_4), and taken to dryness under vacuum. The residue was purified by column chromatography on silica gel (petroleum ether/ethyl acetate 8:2 v/v as eluent) to give 2.50 g (90% yield) of compound **2**.

Step 3: Preparation of Methyl [6,8-Dichloro-2-(1,3-thiazol-2-yl)imidazo[1,2-*a*]pyridin-3-yl]acetate (3). The bromo keto ester **2** (2.00 g, 7 mmol) was added to a solution of 2-amino-3,5-dichloropyridine (1.50 g, 9 mmol) in toluene (40 mL). The reaction mixture was refluxed under stirring for about 48 h; meanwhile, the progress of the reaction was monitored by TLC (petroleum ether/ethyl acetate 8:2 v/v as eluent). When the reaction was complete, the solvent was removed under reduced pressure, and the resulting residue was purified by column chromatography on silica gel (petroleum ether/ethyl acetate 8:2 v/v as eluent) to give 1.4 g (81% yield) of compound **3** as a white solid. Mp 75−80 °C; IR 1728 cm^{-1} ($\nu_{C=O}$); ^{1}H NMR ($CDCl_3$) δ 3.74 (s, 3H, $-OCH_3$), 4.67 (s, 2H, $-CH_2CO$), 7.33 (d, J = 1.6 Hz, 1H, Ar), 7.39 (d, J = 3.3 Hz, 1H, Ar), 7.89 (d, J = 3.3 Hz, 1H, Ar), 7.99 (d, J = 1.6 Hz, 1H, Ar); MS m/z 340.9 (38, M$^+$), 308.9 (base). Anal. ($C_{13}H_9O_2N_3Cl_2S$) C, H, N.

Step 4: Preparation of [6,8-Dichloro-2-(1,3-thiazol-2-yl)-imidazo[1,2-*a*]pyridin-3-yl]acetic Acid (4). HCl (1 N, 5 mL) was added dropwise to a solution of the methyl ester **3** (1.00 g, 3 mmol) in dioxane (20 mL). The mixture was stirred at 50 °C for 24 h and then the solvent was evaporated under reduced pressure. The residue was treated with water (50 mL), and the mixture was washed with ethyl acetate (3 × 20 mL). The cooled aqueous phase was acidified to pH 4 with dilute HCl, and the resulting precipitate, corresponding to pure compound **4**, was isolated by filtration of the mother liquor (55% yield). Mp 205 °C dec; IR 3424 (ν_{O-H}), 1698 ($\nu_{C=O}$) cm^{-1}; ^{1}H NMR (DMSO-d_6) δ 4.58 (s, 2H, $-CH_2CO$), 7.74 (d, J = 1.7 Hz, 1H, Ar), 7.79 (d, J = 3.3 Hz, 1H, Ar), 7.96 (d, J = 3.3 Hz, 1H, Ar), 7.86 (d, J = 1.7 Hz, 1H, Ar); MS m/z 282.9 (base). Anal. ($C_{12}H_7O_2N_3Cl_2S$) C, H, N.

Step 5: Preparation of 2-[6,8-Dichloro-2-(1,3-thiazol-2-yl)*H*-imidazo[1,2-*a*]pyridin-3-yl]-*N*,*N*-dipropylacetamide (5). Ethyl 1,2-dihydro-2-ethoxy-1-quinolinecarboxylate (0.28 g, 1.14 mmol) and dipropyl amine (0.125 mL, 0.92 mmol) were added to a stirred solution of **4** (0.25 g, 0.76 mmol) in anhydrous THF (20 mL). After stirring at room temperature for 10 min, the reaction mixture was treated with triethyl amine added dropwise (0.16 mL, 1.14 mmol). Stirring was continued for an additional 24 h at room temperature, and then the solvent was evaporated under reduced pressure. The resulting residue was purified by column chromatography on silica gel (petroleum ether/ethyl acetate 7:3 v/v as eluent) to give the desired compound **5** as a white solid (65 mg, 20.6% yield). Mp 158−163 °C; IR 1649 ($\nu_{C=O}$) cm^{-1}; ^{1}H NMR ($CDCl_3$) δ 0.82 (t, J = 7.6 Hz, 6H, $-CH_2CH_2CH_3$), 1.4−1.6 (m, 4H, $-CH_2CH_2CH_3$), 3.27 (t, J = 7.6 Hz, 2H, $-CH_2CH_2CH_3$), 3.42 (t, J = 7.6 Hz, 2H, $-CH_2CH_2CH_3$), 4.70 (s, 2H, $-CH_2CON$), 7.31 (d, J = 1.6 Hz, 1H, Ar), 7.39 (d, J = 3.2 Hz, 1H, Ar), 7.86 (d, J = 3.2 Hz, 1H, Ar), 8.60 (d, J = 1.6 Hz, 1H, Ar); MS m/z 410.0 (27, M$^+$), 281.9 (base); MS (ESI) m/z 411.1 [M + H]$^+$. Anal. ($C_{18}H_{20}ON_4Cl_2S$) C, H, N.

Synthesis of Zeise's Salt (6). K[$PtCl_3(\eta^2$-$C_2H_4)$] (Zeise's salt) was prepared according to the method of Chock et al. from potassium tetrachloroplatinate and ethylene gas.[50]

Synthesis of *trans*-[$PtCl_2(C_2H_4)$(5)] (7). Compound **5** (103 mg, 0.25 mmol) was dissolved in methanol (40 mL), and the resulting solution was treated with K[$PtCl_3(\eta^2$-$C_2H_4)$] (92 mg, 0.25 mmol). The yellow solution was stirred in the dark at room temperature for 24 h; meanwhile, a pale yellow precipitate formed. The solid was isolated by filtration of the solution, washed with a few drops of methanol, and dried under vacuum. Compound **7** (168 mg) was obtained (yield = 95%) and characterized by elemental analysis, IR, and NMR spectroscopy. IR 1645.7 ($\nu_{C=O}$), 332.2 (ν_{Pt-Cl}) cm^{-1}. ^{1}H NMR ($CDCl_3$) 0.78−0.88 (m, 6H, $-CH_2CH_2CH_3$), 1.4−1.6 (m, 4H, $-CH_2CH_2CH_3$), 3.24 (t, J = 7.6 Hz, 2H, $-CH_2CH_2CH_3$), 3.33 (t, J = 7.6 Hz, 2 H, $-CH_2CH_2CH_3$), 4.51 (s, 2H, $-CH_2CON$), 4.57 (s with satellites, 4H, ethylene, $^2J_{H-Pt} \sim 60$ Hz), 7.47 (br, 1H, Ar), 7.57 (br, 1H, Ar), 8.04 (br with Pt satellites, $^3J_{H-Pt} \sim 40$ Hz, 1H, Ar), 8.41 (br, 1H, Ar). Anal. Calculated for *trans*-[$PtCl_2(\eta^2$-$C_2H_4)$(**5**)] (compound **7**) ($C_{20}H_{24}Cl_4N_4OPtS$) C, H, N.

Synthesis of *cis*-[$PtCl_2$(5)] (8). Compound **7** containing mono-coordinated **5** can be converted to the species with biscoordinated **5** by spontaneous rearrangement in solution. Hence, compound **7** was dissolved in chloroform, and the resulting solution was placed in an open flask and kept for one week at 50 °C, refilling the solvent when necessary to maintain a constant volume of solvent. The solution was then filtered, and the yellow filtrate was concentrated to dryness. The yellow-orange residue was washed with water, dried under vacuum, and dissolved in acetone (50 mL). The acetone solution was treated with pentane (500 mL) until the incipient formation of a yellow-orange precipitate, and then the mixture was cooled to 5 °C and kept standing for one night. The precipitate

was isolated by filtration of the mother solution, washed with pentane, and dried under vacuum. Compound **8** (126 mg) was obtained (yield = 74% referred to platinum). IR 1639 ($\nu_{C=O}$), 351.8 and 335.2 (ν_{Pt-Cl}) cm^{-1}. ^1H and ^{13}C NMR data are reported in Table 1. Anal. for **8**·$^1/_3CH_3COCH_3$ ($C_{57}H_{66}Cl_{12}N_{12}OPt_3S_3$) C, H, N.

Determination of the Dimerization Constant. Compound **8** undergoes in chloroform solution an association process with formation of a dimeric species. The monomer and the dimer have individual NMR signals that allowed the evaluation of the dimerization constant. Compound **8** (1.5 mg, 2.2×10^{-3} mmol) was dissolved in $CDCl_3$ (2.0 mL) to obtain a final concentration of 1.1×10^{-3} M. An aliquot of this solution (0.8 mL) was transferred into an NMR tube, and the ^1H NMR spectrum was recorded. By the addition of solvent, the concentration of the initial solution was progressively lowered. The NMR spectra of the solutions having different concentrations (1.1×10^{-3}, 8.8×10^{-4}, 7.4×10^{-4}, 5.3×10^{-4}, 3.3×10^{-4}, 2.4×10^{-4}, 1.4×10^{-4}, and 0.7×10^{-4} M) were recorded, and the concentrations of individual species were calculated from integration values.

By assuming a monomer/dimer equilibrium (in slow exchange on the NMR time scale)

$$2M \rightleftharpoons D$$

the equilibrium constant can be expressed as $K = [D]/[M]^2$. If we indicate with I_D the integrated value of a given proton in the dimer (D) and with I_M the integrated value of the corresponding proton in the monomer (M), from the system of the following two eqs, $2[D] + [M] = C_{TOT}$ and $0.5I_D/I_M = [D]/[M]$, it is possible to calculate for each value of C_{TOT} the values of $[M]$ ($[M] = C_{TOT}I_M/(I_D + I_M)$), $[D]$ ($[D] = C_{TOT}I_D/2(I_D + I_M)$), and therefrom the value of K. The evaluated values of K for different values of C_{TOT} (reported in Table 2) are fairly constant and give a mean value of $2.57 (\pm 0.51) \times 10^3$ M^{-1} (mean ± standard deviation from seven experiments).

Determination of Molecular Radii and Diffusion Coefficients. The radii of monomeric **8** and of its dimeric aggregate were calculated from the volume obtained by the gas-phase structures optimized at the PM3 semiempirical level[51] with the software Spartan 02.[32] The theoretical Diff were calculated from the Stokes−Einstein equation: $Diff = (k_BT)/(6\pi\eta r)$, where k_B is the Boltzman constant, T is the temperature in Kelvin, η is the viscosity of the solution, and r is the radius of the molecular sphere. The viscosity of chloroform (0.55425 cP) at the temperature of the DOSY experiments (298 K) was extrapolated from the physical tables reported on the Bruker Almanac.

In Vitro Receptor Binding Assays. Binding assays were performed according to the methods described previously.[24] Briefly, male Sprague−Dawley CD rats at 30 days of age were killed, the brain was rapidly removed, the cerebral cortex was dissected, and all tissues were stored at −80 °C. To perform the assays, the tissues were thawed and homogenized in 50 volumes of Dulbecco's phosphate buffered saline (PBS) at pH 7.4 and 4 °C with a Polytron PT 10 (setting 5, for 20 s). The homogenate was centrifuged at 40 000 × *g* for 30 min, and the resulting pellet was resuspended in 50 volumes of PBS and centrifuged again. The new pellet was resuspended in 10 volumes of PBS and used for the assay. [^3H]PK 11195 binding was determined in a final volume of 500 μL, comprising 50 μL of membrane suspension (0.15−0.20 mg protein), 50 μL of [^3H]PK 11195 (85.5 Ci/mmol, New England Nuclear; final assay concentration 1 M), and 400 μL of PBS buffer (pH 7.4 at 25 °C). Incubation (25 °C) was initiated by the addition of membrane suspensions and was terminated 90 min later by rapid filtration through glass-fiber filter strips (Wathaman GF/B) that had been presoaked with 0.3% polyethyleneimine and placed in a cell harvester manifold (Brandel). The filters were rinsed five times with 4 mL of ice-cold PBS buffer, after which filter-bound radioactivity was quantified by liquid scintillation spectrometry. Nonspecific binding was defined as the binding in the presence of 10 μM of unlabeled PK 11195 (Sigma).

[^3H]Flunitrazepam Binding. Cerebral cortex was homogenized with a Polytron PT 10 in 50 volumes of ice-cold 50 mM Tris-HCl (pH 7.4), and the homogenate was centrifuged twice at 20 000 × *g* for 10 min. The final pellet was reconstituted in 50 volumes of Tris-HCl buffer and used for the binding assay. [^3H]-flunitrazepam binding was determined in a final volume of 1000 μL, comprising 400 μL of membrane suspension (0.4 to 0.5 mg of protein), 400 μL of Tris-HCl buffer, 100 μL of [^3H]-flunitrazepam (74 Ci $mmol^{-1}$; New England Nuclear), and 100 μL of drug solution or solvent. Incubations were performed for 60 min at 0 °C and were terminated by rapid filtration through glass-fiber filter strips (Whatman GF/B). The filters were then rinsed with ice-cold Tris-HCl buffer and filter-bound radioactivity was quantitated by liquid scintillation spectrometry. Nonspecific binding was determined as binding in the presence of 5 μM diazepam and represented about 10% of total binding.

Acknowledgment. The authors thank the Università degli Studi di Bari, the Italian "Ministero dell'Istruzione, Università e Ricerca (MIUR)" (PRIN 2004 n. 2004059078_006), and the EC (COST Chemistry projects D20/0001/2000 and D20/0003/01) for support. The authors are also grateful to Dr. Paride Papadia, Università degli Studi di Lecce, for assistance.

Supporting Information Available: [$^1H-^{13}C$] HETCOR 2D spectrum of compound **5**, [$^1H-^{13}C$] HETCOR, TOCSY, and ROESY 2D spectra of **8**. Elemental analyses of compunds **3**, **4**, **5**, **7**, and **8**. This material is available free of charge via the Internet at http://pubs.acs.org.

References

(1) Lippert, B., Ed. *Cisplatin: Chemistry and Biochemistry of a Leading Anticancer Drug*; Verlag Helvetica Chimica Acta: Zürich, 1999; p 563.
(2) Fuertes, M. A.; Alonso, C.; Pérez, J. M. Biochemical Modulation of Cisplatin Mechanisms of Action: Enhancement of Antitumor Activity and Circumvention of Drug Resistance. *Chem. Rev.* **2003**, *103*, 645−662.
(3) O'Dwyer, P. J.; Stevenson, J. P.; Johnson, S. W. in reference 1.
(4) Cleare, M. J.; Hoeschele, J. D. Antitumor platinum compounds. Relation between structure and activity. *Platinum Met. Rev.* **1973**, *17*, 2−13.
(5) Cleare, M. J.; Hoeschele, J. D. Antitumor activity of Group VIII transition metal complexes. I. Platinum(II) complexes. *Bioinorg. Chem.* **1973**, *2*, 187−210.
(6) Wong, E.; Giandomenico, C. M. Current Status of Platinum-Based Antitumor Drugs. *Chem. Rev.* **1999**, *99*, 2451−2466.
(7) Natile, G.; Coluccia, M. In *Metal ions in biological systems (Metal complexes in tumor diagnosis and as anticancer agents*); Sigel A., Sigel H., Eds.; FontisMedia S.A.: Basel and Marcel Dekker, Inc.: Switzerland, 2004; Vol. 42, pp. 209−250.
(8) Coluccia, M.; Mariggiò, A.; Boccarelli, A.; Loseto, F.; Cardellicchio, N.; Caputo, P.A.; Intini, F.P.; Natile, G. In *Platinum and Other Metal Coordination Compounds in Cancer Chemotherapy*; Pinedo, H. M., Schrnagel, J. H., Eds.; Plenum Press: New York, 1996; pp 27−35..
(9) Wang, D.; Lippard, S. J. Cellular processing of platinum anticancer drugs. *Nat. Rev. Drug Discovery* **2005**, *4*, 307−320.
(10) Galanski, M.; Jakupec, M. A.; Keppler, B. K. Update of the preclinical situation of anticancer platinum complexes: Novel design strategies and innovative analytical approaches. *Curr. Med. Chem.* **2005**, *12*, 2075−2094.
(11) Papadopoulos, V.; Baraldi, M.; Guilarte, T. R.; Knudsen, T. B.; Lacapère, J.-J.; Lindemann, P.; Norenberg, M. D.; Nutt, D.; Weizman, A.; Zhang, M.-R.; Gavish, M. Translocator Protein (18 kDa): New nomenclature for the peripheral-type benzodiazepine receptor based on its structure and molecular function. *Trends Pharmacol. Sci.* **2006**, *27*, 402−409.
(12) Galiegue, S.; Tinel, N.; Casellas, P. The peripheral benzodiazepine receptors a promising therapeutic drug target. *Curr. Med. Chem.* **2003**, *10*, 1563−1572.
(13) Giesen-Crouse, E. In *Peripheral benzodiazepine receptors*; Giesen-Crouse, E., Ed.; Academic Press: London, 1993.
(14) Maaser, K.; Grabowski, P.; Surter, A. P.; Hopfner, M.; Foss, H. D.; Stein, H.; Berger, G.; Gavish, M.; Zeitz, M.; Scherübl, A. P. Overexpression of the peripheral benzodiazepine receptor is a relevant prognostic factor in stage III colorectal cancer. *Clin. Cancer Res.* **2002**, *8*, 3205−3209.

(15) Miettinen, H.; Kononen, J.; Haapasalo, H.; Helen, P.; Sallinen, P.; Harjuntausta, T.; Helin, H.; Alho, H. Expression of peripheral-type benzodiazepine receptor and diazepam binding inhibitor in human astrocytomas: relationship to cell proliferation. *Cancer Res.* **1995**, *55*, 2691−2695.
(16) Veenman, L.; Levin, E.; Weisinger, G.; Leschiner, S.; Spanier, I.; Snyder, S. H.; Weizman, A.; Gavish, M. Peripheral-type benzodiazepine receptor density and in vitro tumorigenicity of glioma cell lines. *Biochem. Pharmacol.* **2004**, *68*, 689−698.
(17) Cappelli, A.; Mohr, G. P.; Gallelli, A.; Giuliani, G.; Anzini, M.; Vomero, S.; Fresta, M.; Porcu, P.; Maciocco, E.; Concas, A.; Biggio, G.; Donati, A. Structure−activity relationships in carboxamide derivatives based on the targeted delivery of radionuclides and boron atoms by means of peripheral benzodiazepine receptor ligands. *J. Med. Chem.* **2003**, *46*, 3568−3571.
(18) Guo, Z.; Gallo, J. M. Selective Protection of 2′,2′-Difluorodeoxycytidine (Gemcitabine). *J. Org. Chem.* **1999**, *64*, 8319−8322.
(19) Guo, P.; Ma, J.; Guo, Z.; Adams, A. L.; Gallo, J. M. Targeted delivery of a peripheral benzodiazepine receptor ligand-gemcitabine conjugate to brain tumors in a xenograft model. *Cancer Chemother. Pharmacol.* **2001**, *48*, 169−176.
(20) Decaudin, D.; Castedo, M.; Nemati, F.; Beurdeley-Thomas, A.; De Pinieux, G.; Caron, A.; Pouillart, P.; Wijdenes, J.; Rouillard, D.; Kroemer, G.; Poupon, M-F. Peripheral Benzodiazepine receptor ligands reverse apoptosis resistance of cancer cells in vitro and in vivo. *Cancer Res.* **2002**, *62*, 1388−1393.
(21) Oudard, S.; Miccoli, L.; Dutrillaux, B.; Poupon, M. F. Targeting the gene of glucose metabolism for the treatment of advanced gliomas. *Bull. Cancer* **1998**, *85*, 622−627.
(22) Trapani, G.; Franco, M.; Ricciardi, L.; Latrofa, A.; Genchi, G.; Sanna, E.; Tuveri, F.; Cagetti, E.; Biggio, G.; Liso, G. Synthesis and binding affinity of 2-phenyl-imidazo[1,2-*a*]pyridine derivatives for both central and peripheral benzodiazepine receptors. A new series of high-affinity and selective ligands for the peripheral type. *J. Med. Chem.* **1997**, *40*, 3109−3118.
(23) Trapani, G.; Franco, M.; Latrofa, A.; Ricciardi, L.; Carotti, A.; Serra, M.; Sanna, E.; Biggio, G.; Liso, G. Novel 2-phenyl-imidazo[1,2-*a*]-pyridine derivatives as potent and selective ligands for peripheral benzodiazepine receptors. Synthesis, binding affinity, and in vivo studies. *J. Med. Chem.* **1999**, *42*, 3934−3941.
(24) Trapani, G.; Laquintana, V.; Denora, N.; Trapani, A.; Lopedota, A.; Latrofa, A.; Franco, M.; Serra, M.; Pisu, M. G.; Floris, I.; Sanna, E.; Biggio, G.; Liso, G. Structure−activity relationships and effects on the neurosteroids synthesis in a series of 2-phenyl-imidazo[1,2-*a*]-pyridine-acetamide peripheral benzodiazepine receptors ligands. *J. Med. Chem.* **2005**, *48*, 292−305.
(25) Gibson, D.; Mansur, N.; Gean, K. F. Preparation, characterization, and antitumor properties of cis-dichlorodiammineplatinum complexes linked to anthraquinones through position number 2. *J. Inorg. Biochem.* **1995**, *58*, 79−88.
(26) Farrell, N. Current status of structure−activity relationships of platinum anticancer drugs: Activation of the trans geometry. *Met. Ions Biol. Syst.* **1996**, *32*, 603−639.
(27) Farrell, N.; Ha, T. T. B.; Souchard, J. P.; Winner, F. L.; Cros, S.; Johnson, N. P. Cytostatic trans-platinum(II) complexes. *J. Med. Chem.* **1989**, *32*, 2240−2241.
(28) Farrell, N. In *Platinum and other metal coordination compounds in cancer chemotherapy;* Howell, S. B., Ed.; Plenum Press: New York, 1991.
(29) Dondoni, A.; Dall'Occo, T.; Forgagnolo, M.; Medici, A.; Pedrini, P. Synthesis of (2,4′-bithiazol-5′-yl)alkanoic acids from silylthiazoles. A new series of potential antiinflammatory agents. *Gazz. Chim. Ital.* **1986**, *116*, 133−136.
(30) ^{1}H NMR spectrum of 1,3-thiazole taken from the world web site at http://www.aist.go.jp/RIODB/SDBS.
(31) ^{1}H-NMR spectrum of *N*,*N*-dibutyl-formamide taken from the web site at http://www.aist.go.jp/RIODB/SDBS.
(32) *SPARTAN 02*; software for Windows platform; Wavefunction, Inc.: 18401 Von Karman Ave., Suite 370, Irvine, CA 92612, 2002.
(33) Albano, V.; Natile, G.; Panunzi, A. Five-coordinate alkene complexes of palladium(II) and platinum(II). *Coord. Chem. Rev.* **1994**, *133*, 67−114.
(34) Cornia, A.; Fabretti, A. C.; Bonivento, M.; Cattalini, L. The bonding of thiazoles to platinum(II) complexes. X-ray crystal structure of *cis*- and *trans*-[Pt(dimethyl sulfoxide)(thiazole)Cl_2]. *Inorg. Chim. Acta.* **1997**, *255*, 405−409.
(35) Houlding, V. H.; Miskowski, V. M. The effect of linear chain structure on the electronic structure of platinum(II) diimine complexes. *Coord. Chem. Rev.* **1991**, *111*, 145−152.
(36) Connick, W. B.; Henling, L. M.; Marsh, R. E.; Gray, H. B. Emission spectroscopic properties of the red form of dichloro(2,2′-bipyridine)-platinum(II). Role of intermolecular stacking interactions. *Inorg. Chem.* **1996**, *35*, 6261−6265.
(37) Osborn, R. S.; Rogers, D. Crystal structure of the red form of 2,2′-bipyridyldichloroplatinum(II). *J. Chem. Soc., Dalton Trans.* **1974**, 1002−1004.
(38) Zimmerman, S. C.; Wu, W.; Zeng, Z. Complexation of nucleotide bases by molecular tweezers with active site carboxylic acids: Effects of microenvironment. *J. Am. Chem. Soc.* **1991**, *113*, 196−201.
(39) Chen, J.-S.; Shirts, R. B. Iterative determination of the NMR monomer shift and dimerization constant in a self-associating system. *J. Phys. Chem.* **1985**, *89*, 1643−1646.
(40) Kato, M.; Kosuge, C.; Yano, S.; Kimura, M. Two-dimensional stacking of dichloro(dipyridophenazine)platinum(II). *Acta Crystallogr., Sect. C: Cryst. Struct. Commun.* **1998**, *C54*, 621−623.
(41) Valentini, M.; Pregosin, P. S.; Rüegger, H. Applications of pulsed field gradient spin-echo measurements to the determination of molecular diffusion (and thus size) in organometallic chemistry. *Organometallics* **2000**, *19*, 2551−2555.
(42) Keresztes, I.; Williard, P. G. Diffusion-ordered NMR spectroscopy (DOSY) of THF solvated *n*-butyllithium aggregates. *J. Am. Chem. Soc.* **2000**, *122*, 10228−10229 and references therein.
(43) $\ln(I/I_0) = -[\gamma^2\delta^2G^2(\Delta-\delta/3)]$Diff, where I is the peak area, I_0 is the peak area in the absence of gradients, γ is the magnetogyric ratio of the observed nucleus, δ is the gradient duration, Δ is the diffusion time, G is the strength of the gradient pulse, and Diff is the diffusion coefficient.
(44) Stejskal, E. O.; Tanner, J. E. Spin diffusion measurements: spin echoes in the presence of a time-dependent field gradient. *J. Chem. Phys.* **1965**, *42*, 288−292.
(45) Beck, S.; Geyer, A.; Brintzinger, H.-H. Diffusion coefficients of zirconocene-borate ion pairs studied by pulsed field-gradient NMR-evidence for ion quadruples in benzene solutions. *Chem. Commun.* **1999**, 2477−2478 and references therein.
(46) Swierczynski, D.; Luboradzki, R.; Dolgonos, G.; Lipkowski, J.; Schneider, H.-J. Noncovalent interactions of organic halogen compounds with aromatic systems—analyses of crystal structure data. *Eur. J. Org. Chem.* **2005**, 1172−1177.
(47) Romaniewska, A.; Jasztold-Howorko, R.; Regiec, A.; Lis, T.; Kuduk-Jaworska, J. Synthesis, structure and characterization of new olivacine derivatives and their platinum(II) complexes. *Eur. J. Inorg. Chem.* **2003**, 4043−4054.
(48) Price, W. S. Pulsed-field gradient nuclear magnetic resonance as a tool for studying translational diffusion: Part 1. Basic theory. *Concepts Magn. Reson.* **1997**, *9*, 299−336.
(49) Johnson, C. S., Jr. Diffusion ordered nuclear magnetic resonance spectroscopy: Principles and applications. *Prog. Nucl. Magn. Reson. Spectrosc.* **1999**, *34*, 203−256.
(50) Chock, P. B.; Halpern, J.; Paulik, F. E. Potassium trichloro(ethene)-platinate(II) (Zeise's salt). *Inorg. Synth.* **1990**, *28*, 349−351.
(51) Stewart, J. J. P. Optimization of parameters for semiempirical methods I. Method. *J. Comput. Chem.* **1989**, *10*, 209−220.

JM0612160